Contents

S1 Supplementary Figures

On the use of tail-based coincidence metrics as oppossed to correlations-based metrics

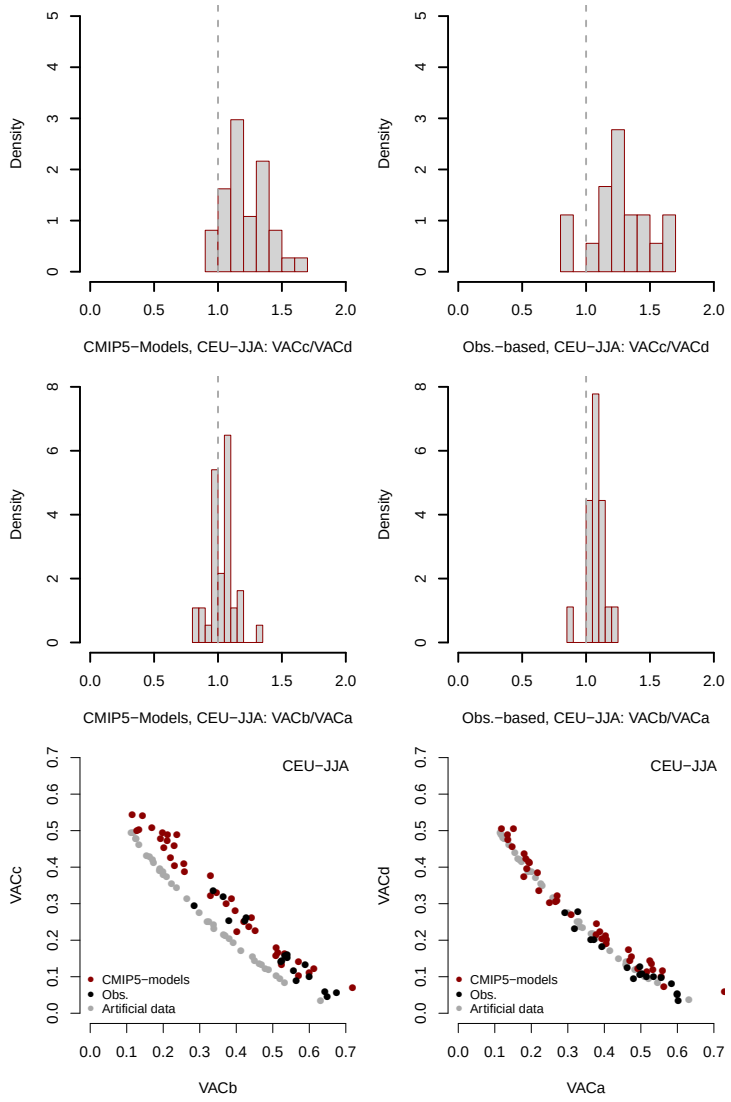

Figure S1. (Top) Ratio of VAC_c/VAC_d occurrences in CMIP5 models (left) and observations (right). (Middle) Ratio of VAC_b/VAC_a occurrences in CMIP5 models (left) and observations (right). (Bottom) Comparison of VAC_b/VAC_c occurrences (left) and VAC_a/VAC_d occurrences (right) in models, observations and artificial data. More frequent occurrences of VAC_c than would be expected in a symmetric dependence structure (as diagnosed e.g. by correlation-based metrics) indicate that the application of coincidences is appropriate.

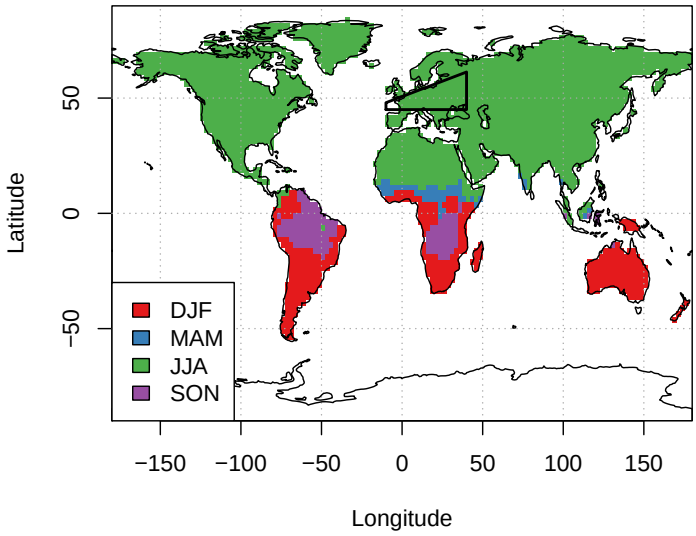

Figure S2. Definition of “warm season" in this study based on long-term seasonal temperatures in the CRU dataset.

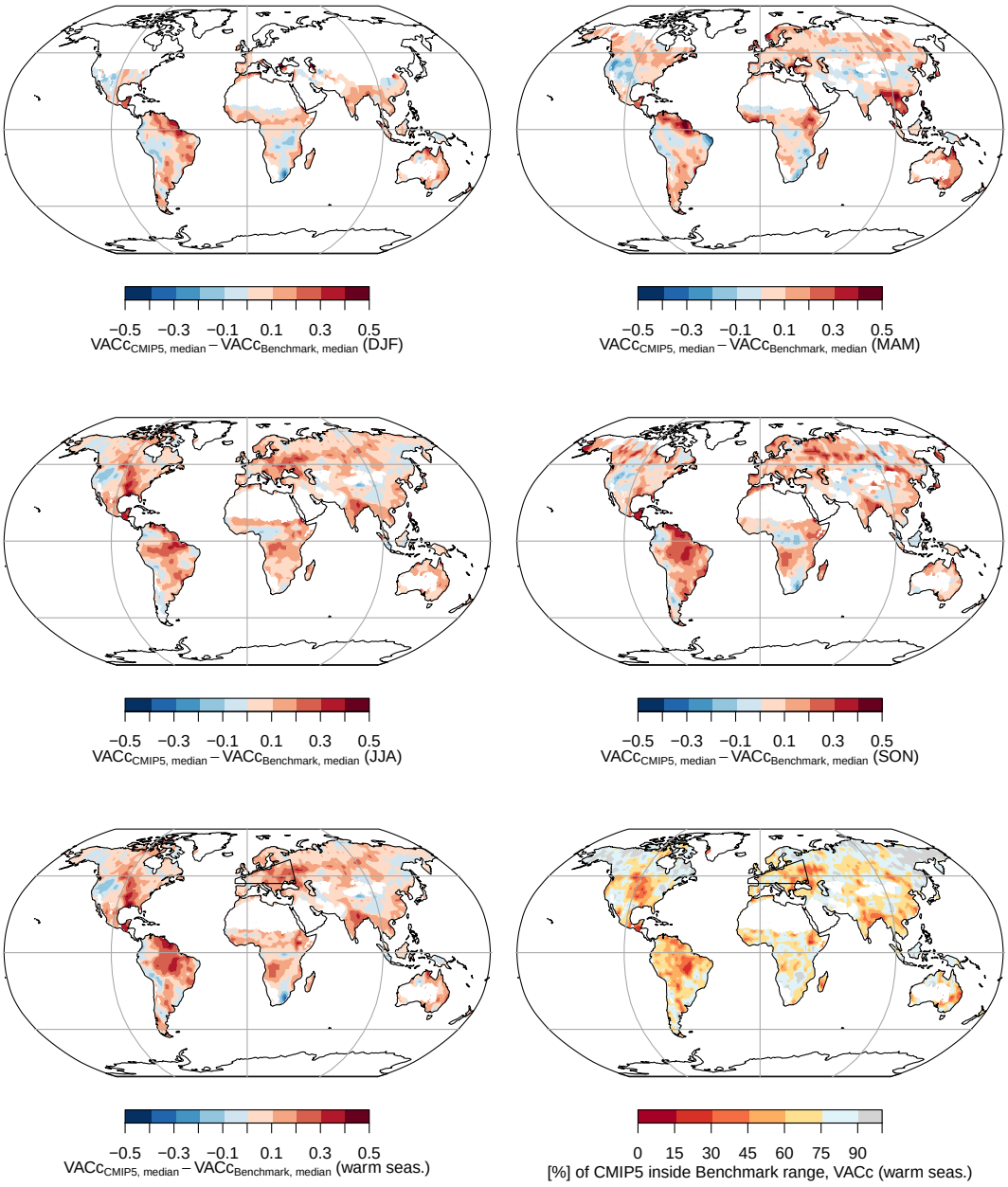

Figure S3. Difference in median VAC_c in CMIP5 models and observations in (top left) DJF, (top right) MAM, (middle left) JJA, and (middle right) SON, the warm season (bottom left). (Bottom right) Fraction of models that are within the 5th to 95th percentile of the ensemble of observations in the warm season (VAC_c).

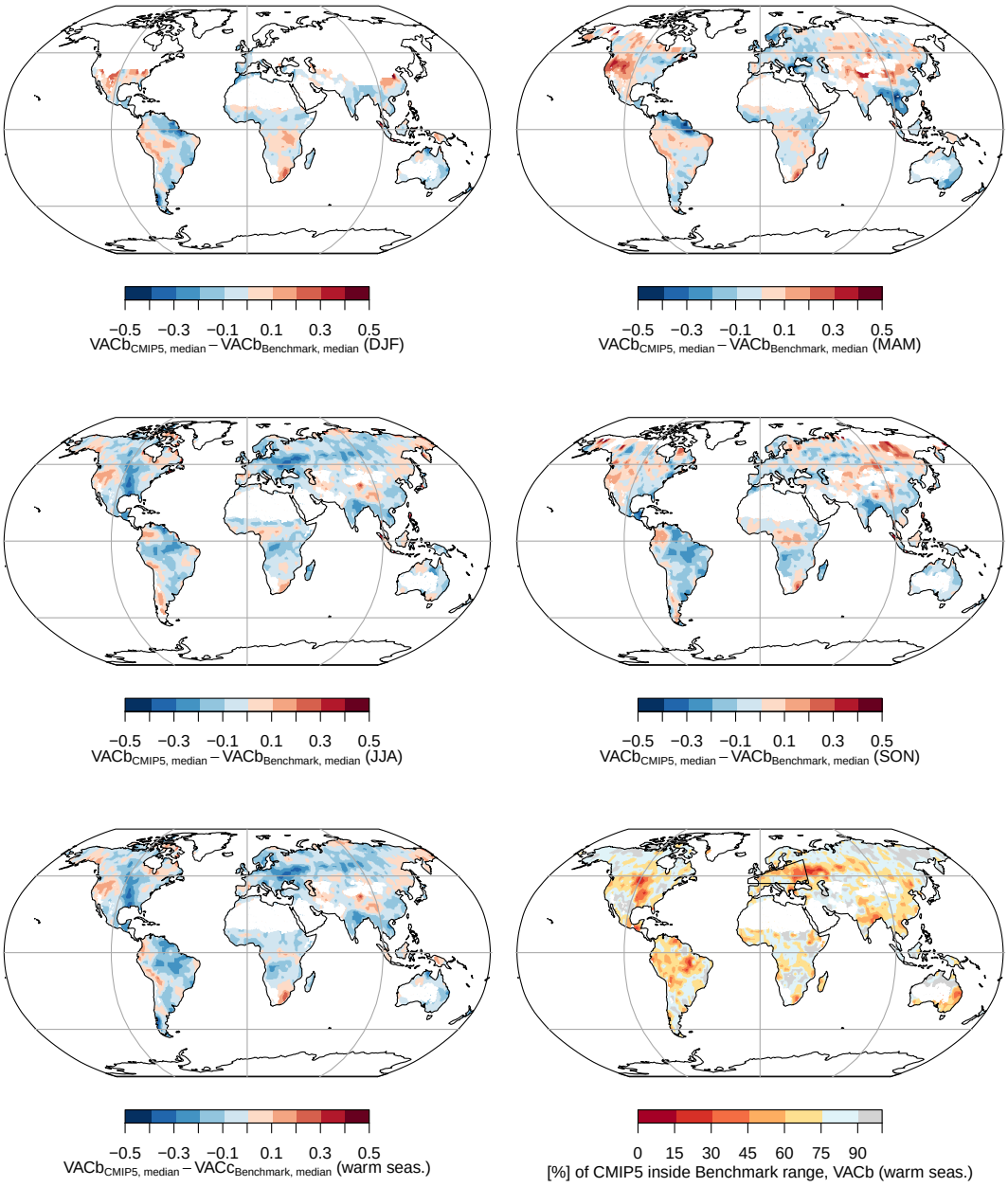

Figure S4. Difference in median VAC_b in CMIP5 models and observations in (top left) DJF, (top right) MAM, (middle left) JJA, and (middle right) SON, the warm season (bottom left). (Bottom right) Fraction of models that are within the 5th to 95th percentile of the ensemble of observations in the warm season (VAC_b).

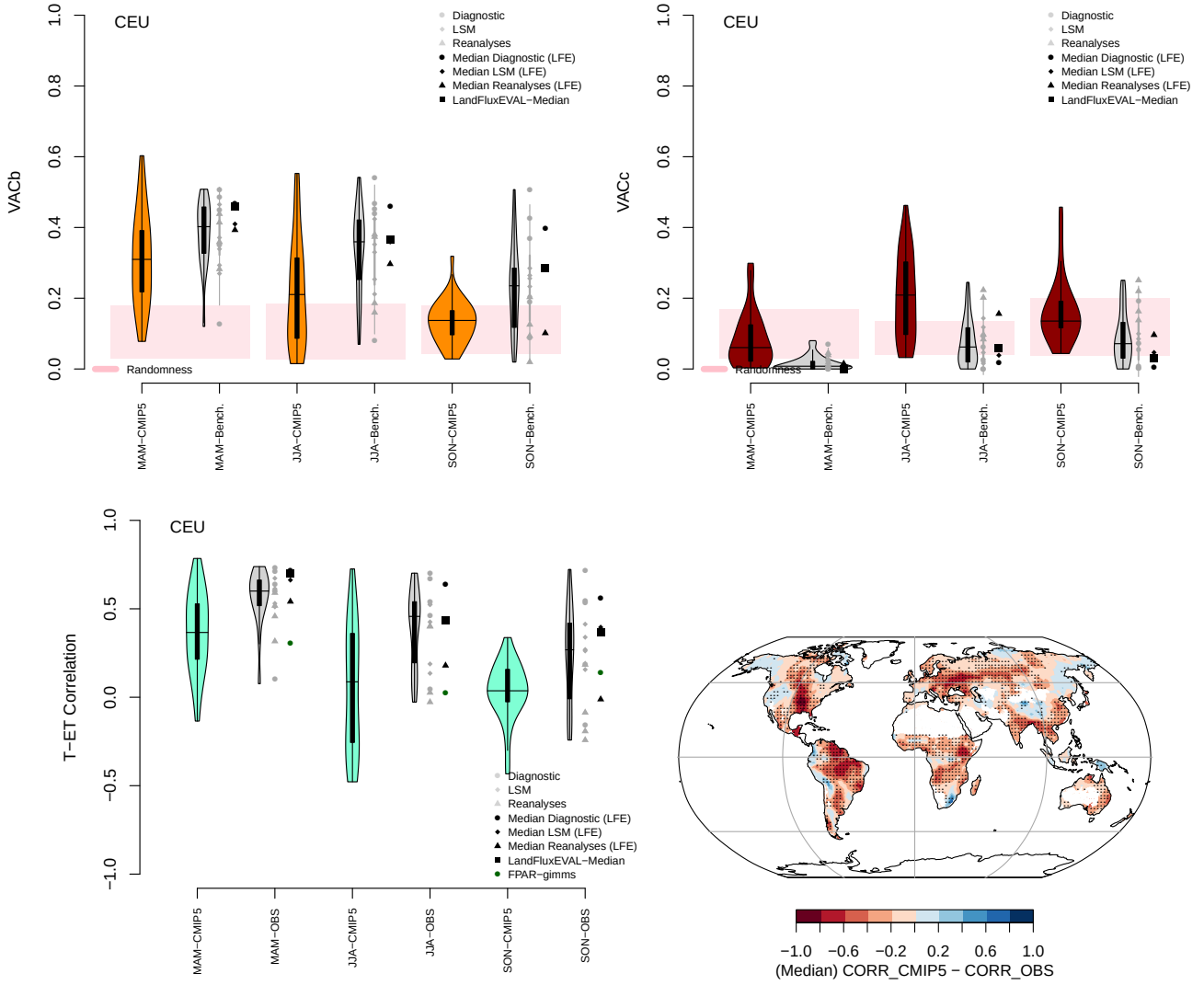

Figure S5. Land-atmosphere coupling in Central Europe in CMIP5 models and observations as diagnosed through (top left) $VACb$ and (top right) $VACc$ based on 90th percentile thresholds, and (bottom left) the Pearson correlation of T and ET anomalies. (Bottom right) Difference in median Pearson corrrelation in CMIP5 models and observations in the warm season.

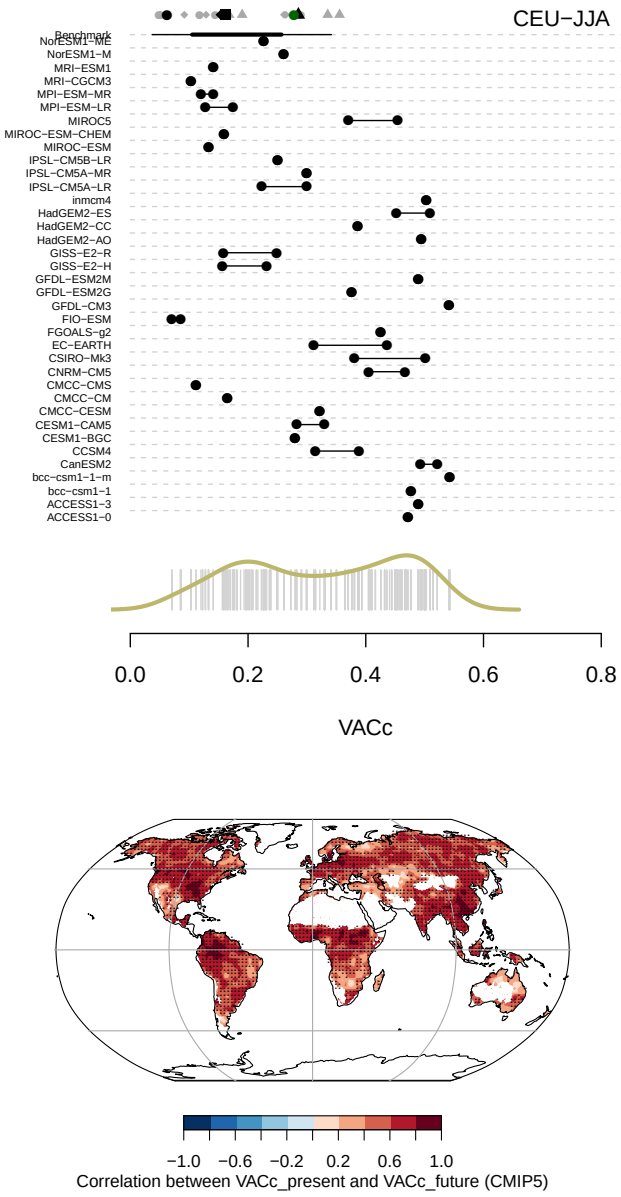

Figure S6. (Top) VAC_c occurrences in Central Europe (JJA) in individual models. (Bottom) Correlation between present-day and future land-atmosphere coupling reveal that occurrences of VAC_c are largely model-inherent features.

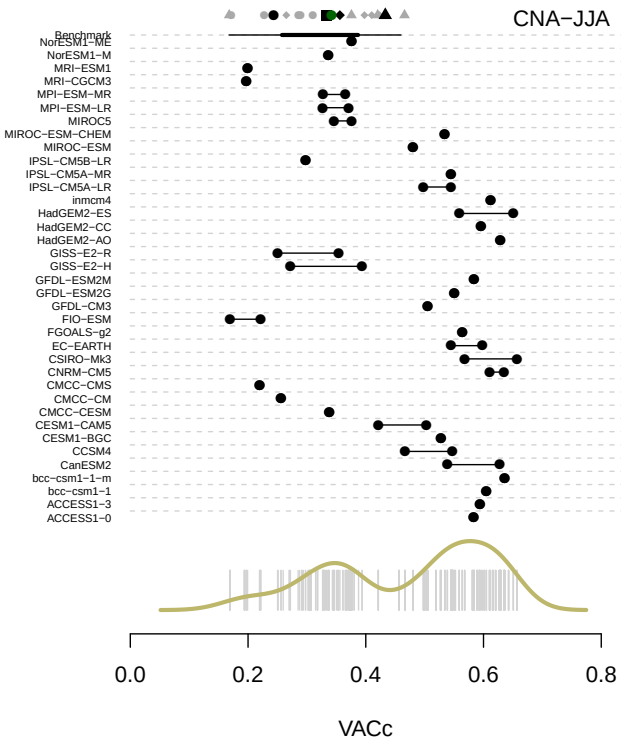

Figure S7. VAC_c occurrences in Central North America (JJA) in individual models.

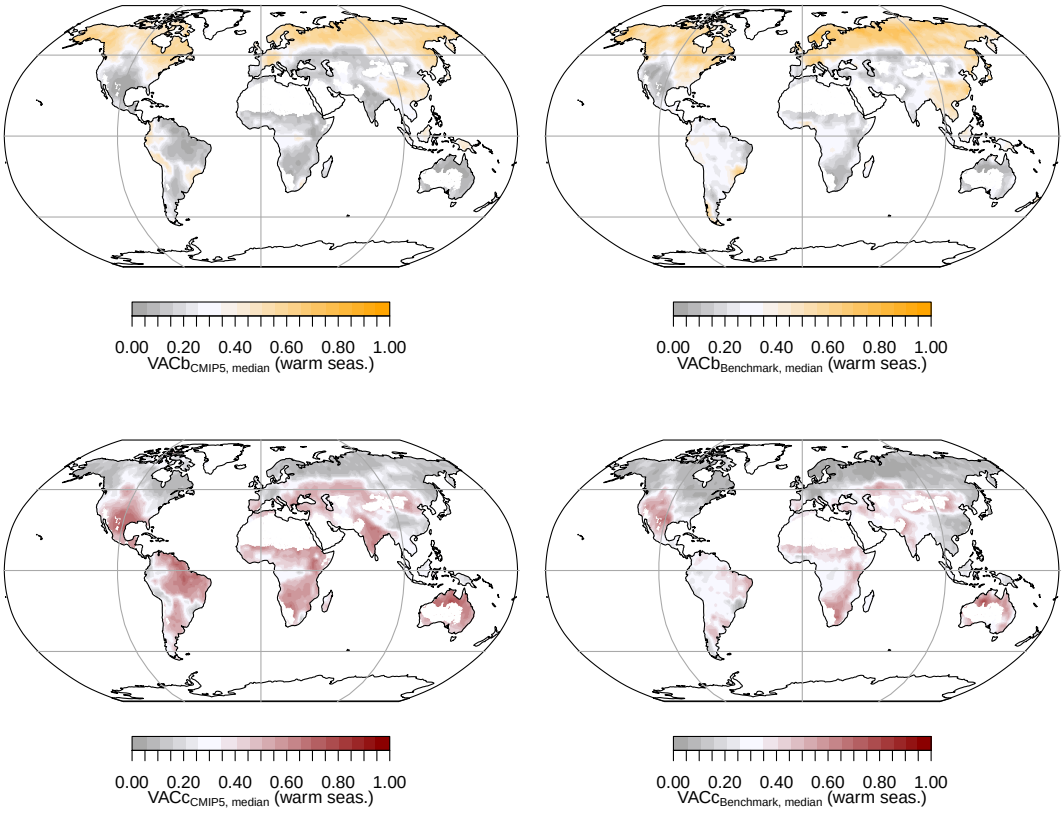

Figure S8. Global patterns in land-atmosphere coupling as diagnosed through (top) VAC_b and (bottom) VAC_c: ensemble median VAC_b/VAC_c in CMIP5 models (left) and ensemble median of the observations-based datasets (right).

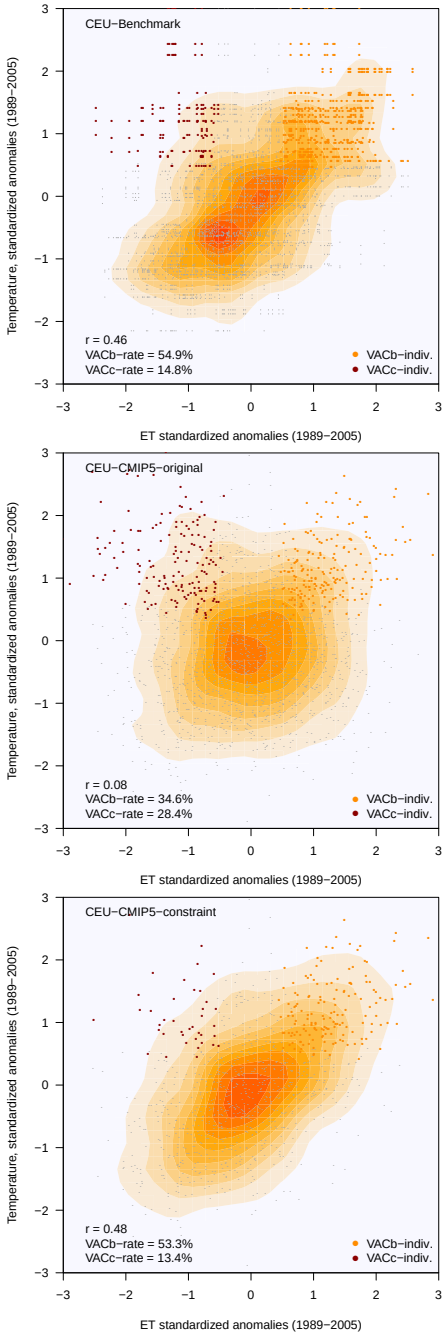

Figure S9. Bivariate kernel density estimates of T-ET relationship in Central Europe in the observations-based benchmarking datasets (Top), the original (middle) and constrained (bottom) CMIP5 ensemble.

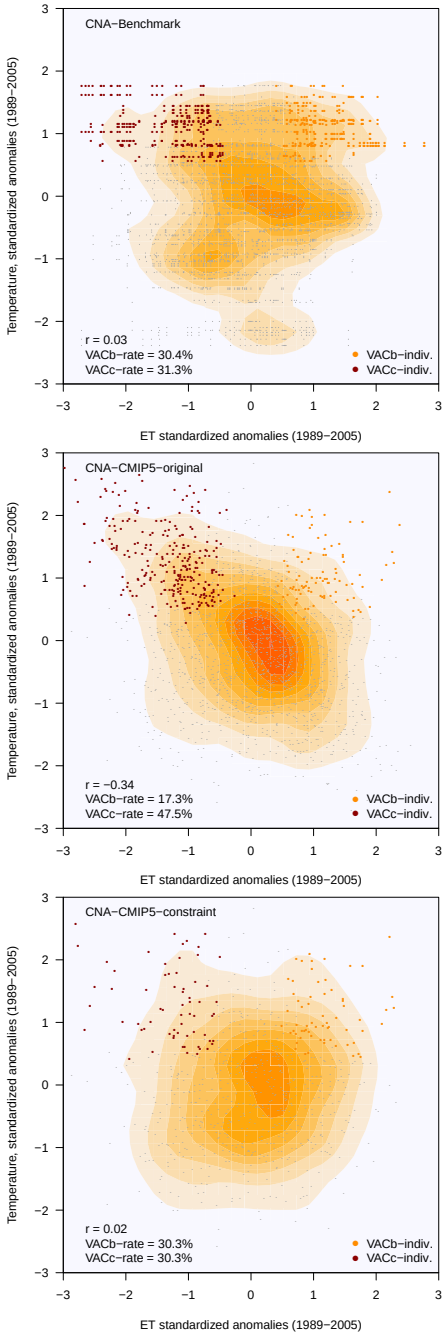

Figure S10. Bivariate kernel density estimates of T-ET relationship in Central North America in the observations-based benchmarking datasets (Top), the original (middle) and constrained (bottom) CMIP5 ensemble.

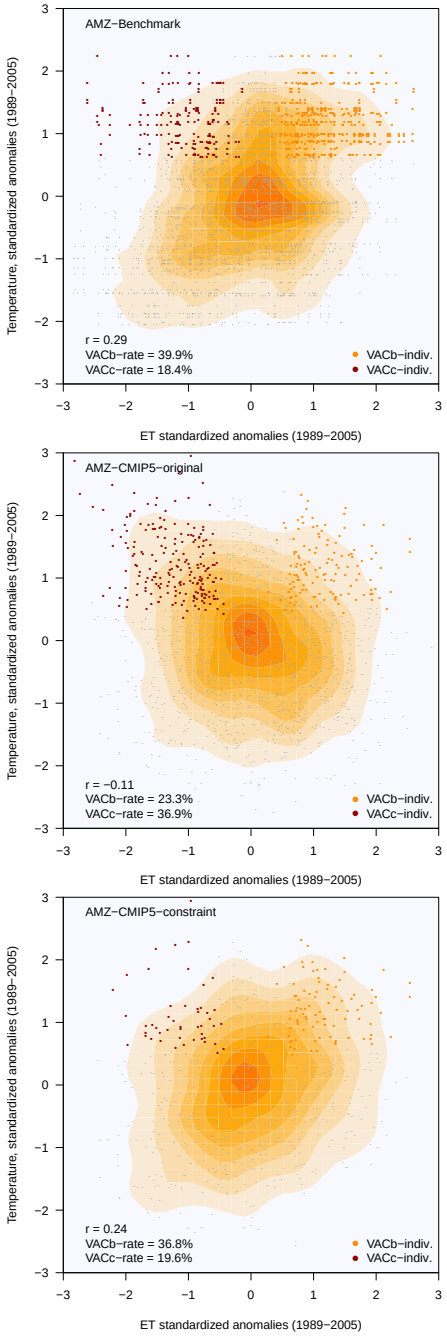

Figure S11. Bivariate kernel density estimates of T-ET relationship in the Amazon region in the observations-based benchmarking datasets (Top), the original (middle) and constrained (bottom) CMIP5 ensemble.

Is there a link between VAC-diagnosed land-atmosphere coupling and (absolute) precipitation or evapotransiration fluxes?

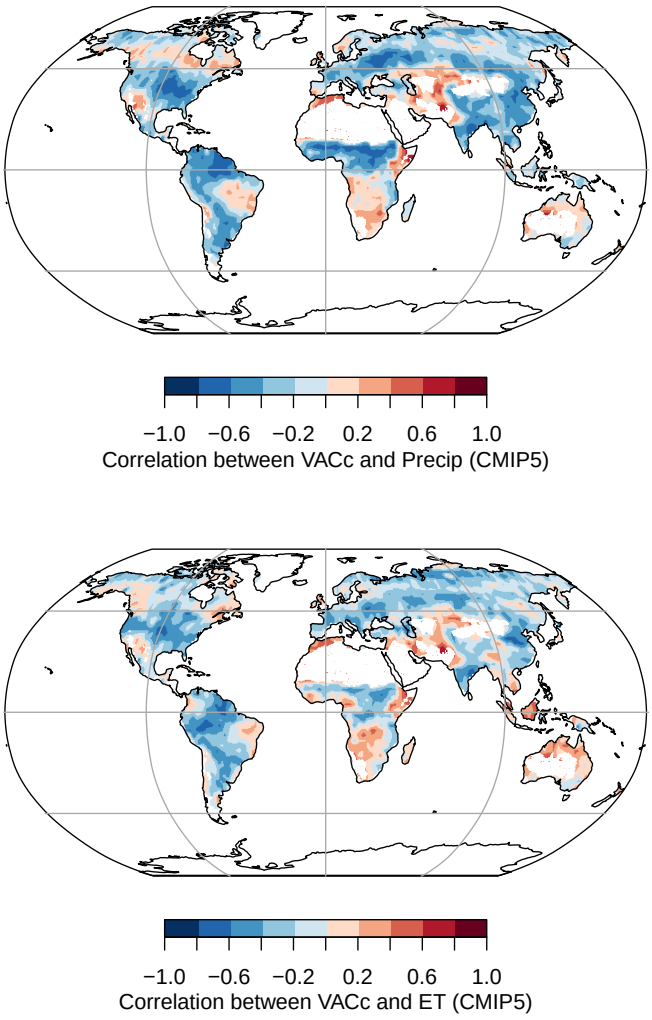

Figure S12. Pearson correlation between (top) VAC_c and rainfall, and (bottom) VAC_c and evapotranspiration across the CMIP5 multi-model ensemble.

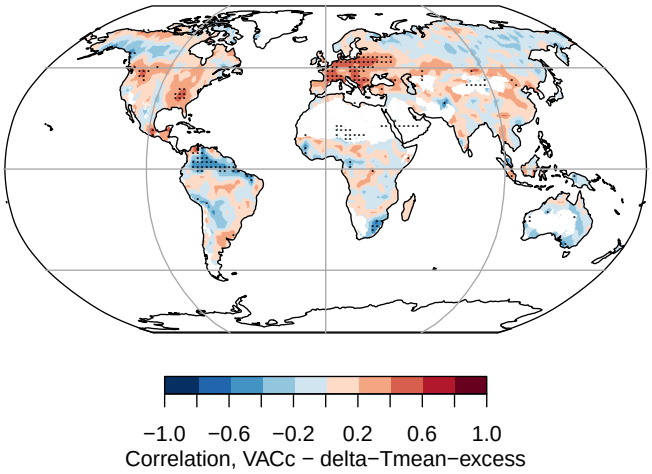

Figure S13. Correlation between VAC_c and the "excess" warming in the warm season (difference between warm season warming and annual mean warming). In boreal regions, the "summer excess warming", is not related to VAC_c.

S2 Supplementary Tables

Table S1. CMIP5 models used for analysis

Model name	Variable	Ensemble member	Scenario
ACCESS1-0	T, ET, TXx	r1i1p1	Historical, RCP8.5
ACCESS1-3	T, ET, TXx	r1i1p1	Historical, RCP8.5
bcc-csm1-1	T, ET, TXx	r1i1p1	Historical, RCP8.5
bcc-csm1-1-m	T, ET, TXx	r1i1p1	Historical, RCP8.5
CanESM2	T, ET, TXx	r1i1p1	Historical, RCP8.5
CCSM4	T, ET, TXx	r1i1p1	Historical, RCP8.5
CESM1-BGC	T, ET, TXx	r1i1p1	Historical, RCP8.5
CESM1-CAM5	T, ET, TXx	r1i1p1	Historical, RCP8.5
CMCC-CESM	T, ET, TXx	r1i1p1	Historical, RCP8.5
CMCC-CM	T, ET, TXx	r1i1p1	Historical, RCP8.5
CMCC-CMS	T, ET, TXx	r1i1p1	Historical, RCP8.5
CNRM-CM5	T, ET, TXx	r1i1p1	Historical, RCP8.5
CSIRO-Mk3	T, ET, TXx	r1i1p1	Historical, RCP8.5
EC-EARTH	T, ET, TXx	r2i1p1	Historical, RCP8.5
FGOALS-g2	T, ET, TXx	r1i1p1	Historical, RCP8.5
FIO-ESM	T, ET	r1i1p1	Historical, RCP8.5
GFDL-CM3	T, ET, TXx	r1i1p1	Historical, RCP8.5
GFDL-ESM2G	T, ET, TXx	r1i1p1	Historical, RCP8.5
GFDL-ESM2M	T, ET, TXx	r1i1p1	Historical, RCP8.5
GISS-E2-H	T, ET, TXx	r6i1p1	Historical, RCP8.5
GISS-E2-R	T, ET, TXx	r6i1p1	Historical, RCP8.5
HadGEM2-AO	T, ET, TXx	r1i1p1	Historical, RCP8.5
HadGEM2-CC	T, ET, TXx	r1i1p1	Historical, RCP8.5
HadGEM2-ES	T, ET, TXx	r1i1p1	Historical, RCP8.5
inmcm4	T, ET, TXx	r1i1p1	Historical, RCP8.5
IPSL-CM5A-LR	T, ET, TXx	r1i1p1	Historical, RCP8.5
IPSL-CM5A-MR	T, ET, TXx	r1i1p1	Historical, RCP8.5
IPSL-CM5B-LR	T, ET, TXx	r1i1p1	Historical, RCP8.5
MIROC-ESM	T, ET, TXx	r1i1p1	Historical, RCP8.5
MIROC-ESM-CHEM	T, ET, TXx	r1i1p1	Historical, RCP8.5
MIROC5	T, ET, TXx	r1i1p1	Historical, RCP8.5
MPI-ESM-LR	T, ET, TXx	r1i1p1	Historical, RCP8.5
MPI-ESM-MR	T, ET, TXx	r1i1p1	Historical, RCP8.5
MRI-CGCM3	T, ET, TXx	r1i1p1	Historical, RCP8.5
MRI-ESM1	T, ET, TXx	r1i1p1	Historical, RCP8.5
NorESM1-M	T, ET, TXx	r1i1p1	Historical, RCP8.5
NorESM1-ME	T, ET	r1i1p1	Historical, RCP8.5